

# Analyzing Straylight X-ray Binaries with NuSTAR

Catherine Slaughter

Fiona Harrison, Brian Grefenstette, and Renee Ludlam

## Abstract

The Nuclear Spectroscopic Telescope ARray (NuSTAR) is the first space telescope to focus hard X-ray bandpass (3-79 keV). NuSTAR was designed to have a deployable mast that is open to the space around it. This means that stray photons from objects that lie 1-4° from the line of sight can fall on the detectors without first going through the optics. Many of these serendipitous straylight observations have been taken over the past eight years, but have not yet been used for research purposes, despite containing a potential wealth of useful data. This project is two-fold. First, I loosely recreate the results of a Homan et al. 2018 paper, which looks at source GX5-1 with focused NuSTAR observations. This serves as a proof-of-concept for the efficacy of straylight research and gives us the opportunity to test the data reduction code written by Brian Grefenstette. Secondly, I perform new time series and spectral analysis on Z-source GX17+2. In particular, use the shape of an iron-line spectral reflection feature (around 6.4-6.97 keV) to determine values for the innermost stable circular orbit of the neutron star binary system's accretion disk.

## 1 Introduction

### 1.1 Motivation

Neutron stars are relatively small, but extremely dense objects that are formed at the end of a massive star's lifetime. They are composed primarily of densely packed neutrons and can create extreme environments that lend themselves to particularly interesting physics. Often, these stars are joined by companion stars of some type, creating a neutron star binary system.

It is often the case with these systems that, due to the high density of the neutron star, it is able to actively accrete material from its companion, forming a disk of material circling the neutron star. The process of accreting this material, in such an extreme environment, is very energetic, and causes the system to release very high-energy x-ray light.

The rate of accretion—and the light output—are not always constant, however. This can be seen on a hardness-intensity diagram. Such a diagram plots the brightness of the system on the x-axis, and the hardness (which is similar to color) of the system on the y-axis. On these diagrams, many neutron star binaries will trace out specific patterns over time (Hasinger and van der Klis, 1989). In general, there are two types of neutron star x-ray binaries, based on the patterns they trace—atoll sources and z-track sources (see fig.3 for an example z-track).

Because these sources are always changing, it can be difficult to observe them in energetic transient states. This means that the more time spent observing a given source, the better. One way researchers can find more data on a given source is by utilizing accidental straylight data from NuSTAR.

## 1.2 Background on NuSTAR

Fiona Harrison is the PI on the Nuclear Spectroscopic Telescope ARray (NuSTAR) satellite, the first focusing space telescope to observe in the "hard" X-ray bandpass (3–79 keV). The group is in charge of daily operations of NuSTAR, as well as analyzing data as it comes down from the satellite. The observational data taken by NuSTAR has a variety of applications within high-energy astrophysics, including research in black holes, neutron stars, and supernovae.

## 1.3 Straylight Observations

NuSTAR's design includes a deployable mast that is "open" to the space around the craft (Harrison et al., 2013). This design means that sometimes, stray light from objects that lie  $1 - 4^\circ$  away from the intended line of sight (see fig.1) can fall on to the detectors of the

scope, without going through the optics (Madsen et al., 2017b). This means that in the 8 years since its launch, NuSTAR has made many thousands of these serendipitous straylight observations. These accidental data potentially contain a wealth of information that may be used in research.

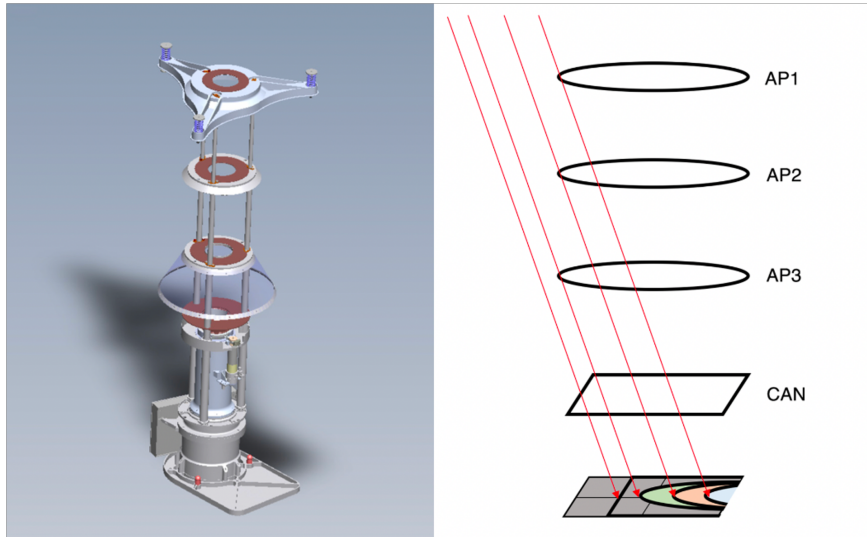


Figure 1: An illustration of how straylight observations are made with NuSTAR. Diagrams taken from instrumentation paper Madsen et al. (2017a).

## 2 Data and Methods

### 2.1 Data Processing

We used data from the NuSTAR flight archive and reprocessed it using the latest HEASOFT and CALDB versions (to account for any updates to the instrument calibration). This process is the same as what would be done with a focused-light NuSTAR observation.

### 2.2 Data Selection

We chose two well known X-ray binaries, GX 5-1 and GX 17+2 for this analysis. For each, we searched through the known straylight observations in the archive to find strong straylight.

In particular, we were looking for observations where the straylight from the source covered a large portion of the field of view, and was not overlapped by other straylight regions or focused sources. An example is seen in fig.2.

For GX5-1, we ended up with 6 different observations with a total exposure time of about a day. When selecting our second target, we went with GX17+2 because it had several particularly long observations. We chose two straylight observations, with a total exposure time of about 253 kilo-seconds, or just under 3 days.

### 2.3 Data Reduction

Using DS9 and a python Jupyter notebook written by Grefenstette, we selected the straylight region (fig.2. Using this and tools from the nustar\_gen python module, we extracted the data from the region areas, and created light curves and spectra for each.

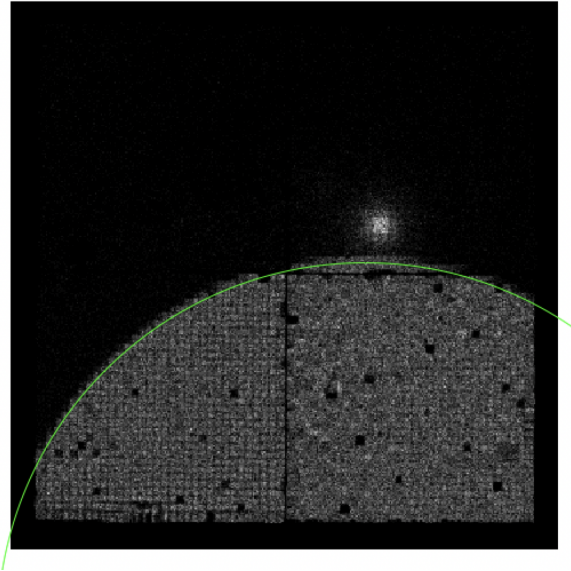


Figure 2: One of the two straylight observations used in my initial analysis. The region used is outlined in green. The bright source above the straylight region was the original intended object for observation.

## 3 Results

### 3.1 GX5-1

We began by attempting to recreate the results of Homan et al. (2018). This paper used focused observations of Z-source GX5-1, taken over the course of several days. They were able to observe the entire z-track of the source, divided the data into several characteristic branches, and performed spectral analysis on each. Our work with GX5-1 was primarily to validate our data processing procedures (outlined in sec. 2). The goal was that our analysis yielded similar results and values to those found in Homan et al. (2018).

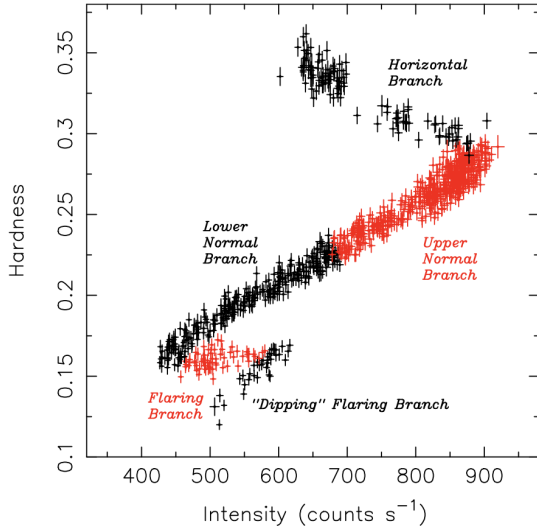


Figure 3: The Hardness-Intensity Diagram from Homan et al. (2018). Note the distinct Z shape in the data.

#### 3.1.1 Light Curves

We began by plotting a hardness-intensity diagram (fig.4) of two of our chosen observations. These two observations only trace out one branch of the expected z-track, so we added the four additional observations (fig.5). From these six seqIDs, we were able to trace out a partial Z-track on the hardness-intensity diagram with two possible branches (see fig.5). As done

in Homan et al. (2018), we analyzed the data sets from the different branches separately (fig.3), because we expect the models to have different parameter values at different times in the z-track.

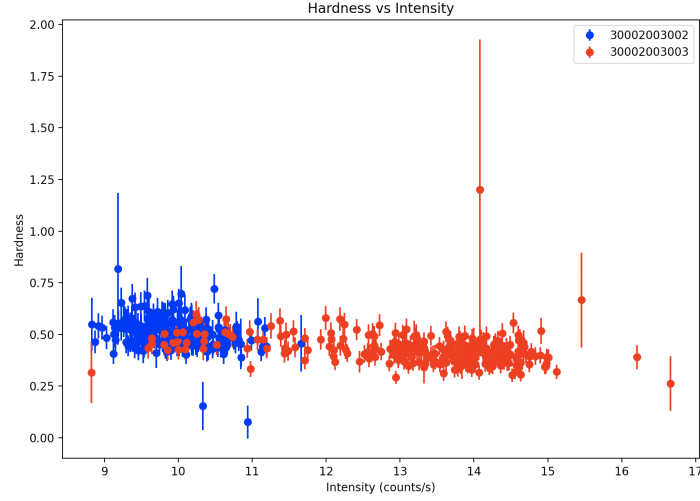


Figure 4: The Hardness-Intensity diagram of the initial two observational data sets used. The sequence IDs for each observation are labeled in the upper right hand corner.

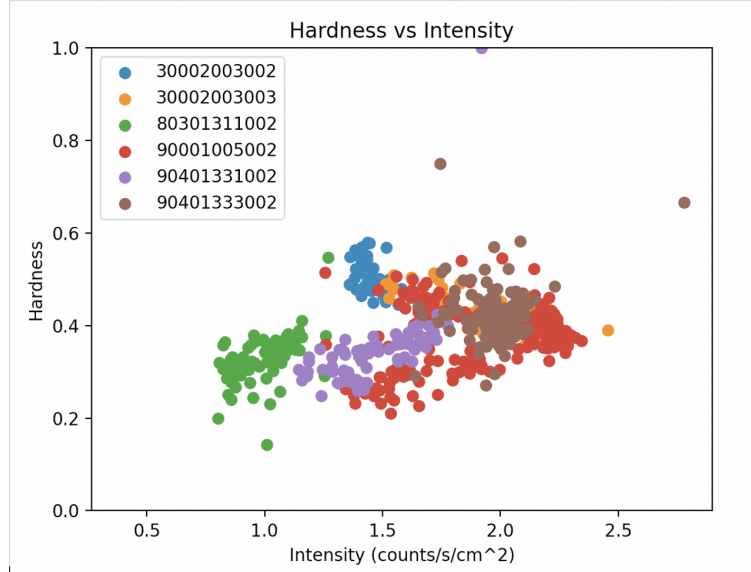


Figure 5: The Hardness-Intensity Diagram of GX5-1. Note the partial Z-track traced out

### 3.1.2 Spectral Modeling

We began by fitting a model to the spectrum continuum for each of the observed z-track branches. The model used for each is a combination of disk blackbody, blackbody radiation from the neutron star itself, and cutoff power law model components (fig.6). By looking at the residual plot for the model, we are able to look more closely for key spectral features. In particular, we're looking for an iron-line reflection feature around 6.4-7.0 keV. As was the case in Homan et al. (2018) and in our initial stray light analysis, no iron-line reflection feature could be found.

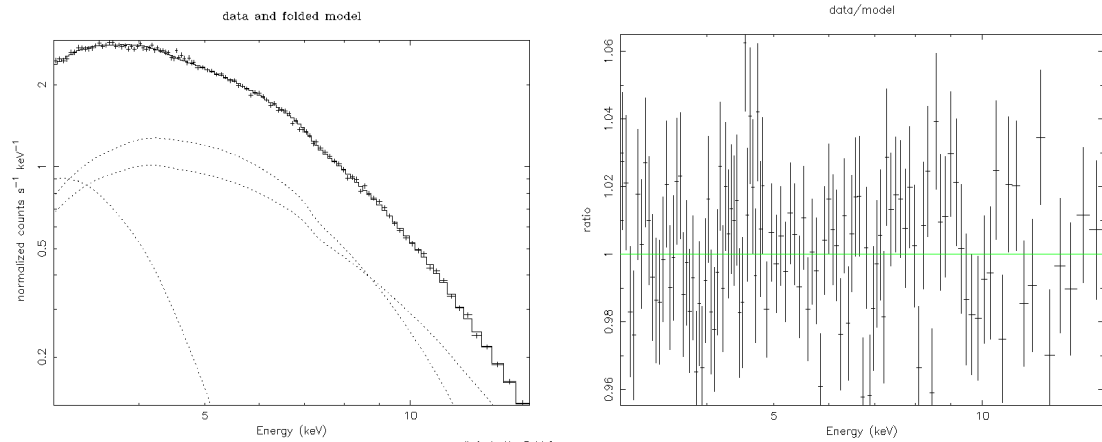


Figure 6: An example spectral data and model (left) and corresponding residual plot (right). The three dotted lines below the spectrum (left) represent the individual diskbb, bbodyrad, and cutoffpl models. On the residual plot (right), no evidence of a spectral line around 6.4-7.0 keV can be seen.

### 3.1.3 Summary

One primary result of the Homan et al. (2018) paper was that the spectral data of GX5-1 did not show evidence of reflection features typically seen in these sources. In particular, this would look like an Fe spectral line around 6.4-7.0 keV. The paper describes several reasons why this feature may not have been observed. Our analysis was able to recreate this result, further indicating that our straylight data reduction was working properly.

By comparing the parameters of the created model to those from Homan et al. (2018) for the horizontal and flaring branches, we could, in principle, determine what section of the z-track these data are in. At this point, however, we felt we had completed our initial proof-of-concept for the efficacy of these straylight observations.

Overall, we were able to achieve a similar model to that created with focused observations, and confirmed the Homan et al. (2018) result that there is no clear iron-line reflection feature from this source. By recreating these results, we show the efficacy of straylight research and that it can be comparable to focused observations for certain analyses. Given the extensive analysis of GX5-1 in Homan et al. (2018), we decided it would be best to move on to our next target.

### 3.2 GX17+2

GX17+2, like GX5-1, is a luminous low-mass neutron star x-ray binary. It is one of many similar sources from which serendipitous stray-light observations have been taken in the past 8 years. We chose to study this source because it had two particular observations (seqIDs 30201034002 and 40501006002) with several hundreds of kiloseconds of exposure time.

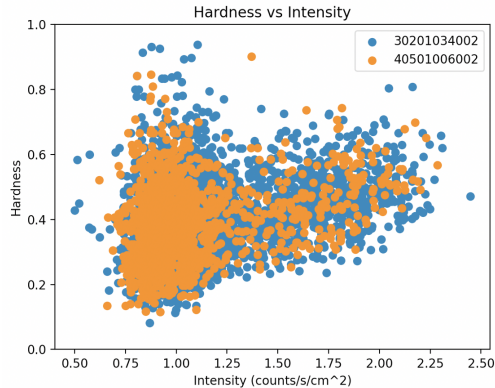


Figure 7: The hardness-intensity diagram for GX17+2. Note the distinct break between the two areas of data at an intensity around 1.3 counts/s/cm<sup>2</sup>. The vertex area is on the left, and the flaring branch area on the right

### 3.2.1 Light Curves

The hope for GX17+2 was that an increased amount of continuous exposure would give us something interesting on the hardness-intensity diagram for the source (see fig.7). We find that for both sets of data, the HID produced can be divided into two broad areas, the Flaring Branch of the z-track, and the vertex. These data are separated so we can perform spectral analyses of each of the two areas of data for each of the two SeqIDs.

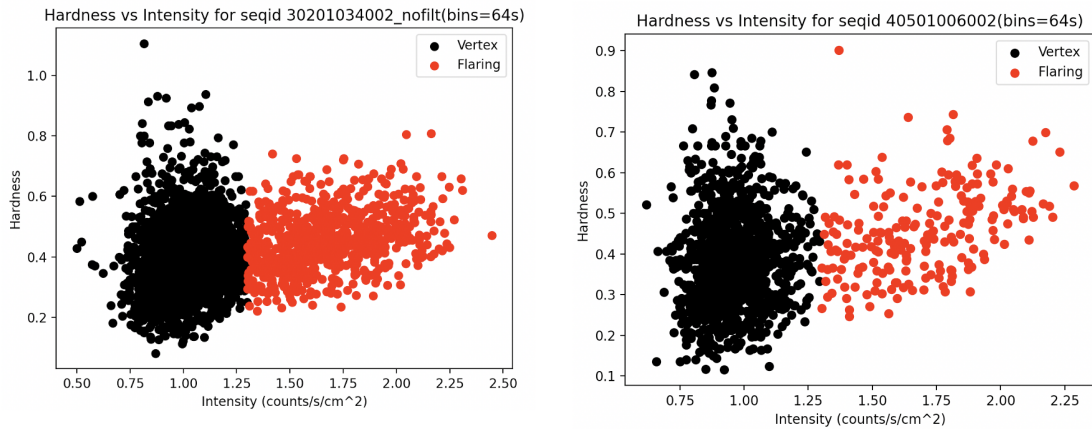


Figure 8: The HIDs for sequence IDs 30201034002 (top) and 40501006002 (bottom), with the separated data sets labelled accordingly.

### 3.2.2 Spectral Modeling

The simpler of the two observations, the data set from seqID 40501006002 was easily divided into its separate areas (fig.8), and the spectra from each area was similar to what we expected.

As for GX5-1, we began by creating very simply continuum models. There appeared to be a fairly clear iron-line reflection feature present in the vertex data, but not so much in the flaring branch data. This is not unexpected, there are several reasons the line strength would be diminished while to source is flaring. It is possible the iron is mostly ionized, for example.

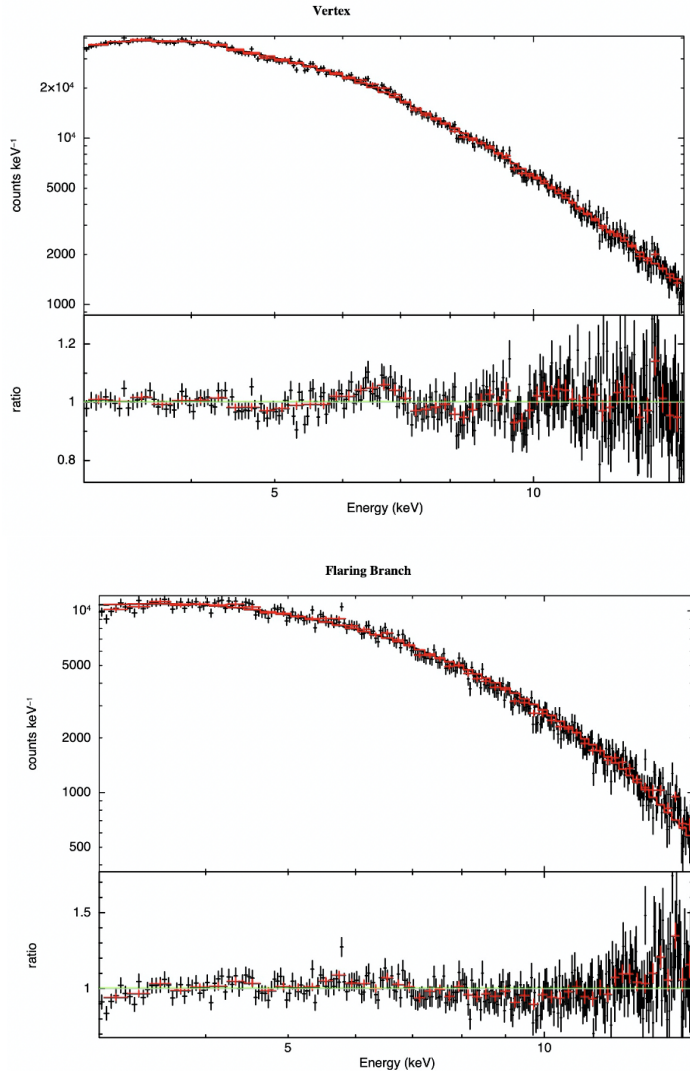


Figure 9: The spectra and their residual plots for the areas of seqID 40501006002. Note the clear iron line around 6-7keV in the vertex (left) spectrum, which is not there in the flaring branch (right) spectrum

Of the two data sets, seqID 30201034002 was the more complicated. As with seqID 40501006002, we began by splitting the data set into its two separate areas, and creating a spectrum from each.

This time, however, we noticed several interesting features in the source's spectra. First, the iron line in the vertex branch appeared much larger than before, and the flaring branch showed an iron line, which was not the case in the previous sequence ID. This alone is not

necessarily nor particularly strange. On the flaring branch, however, we find a feature of unknown origin around 3-4keV.

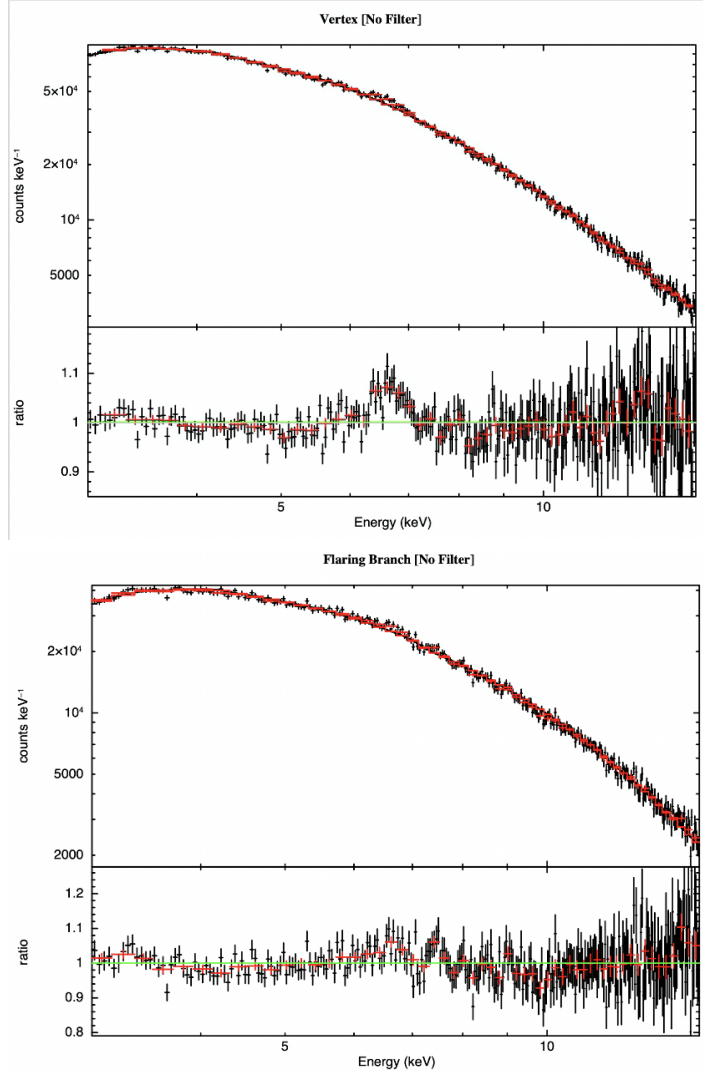


Figure 10: The vertex and flaring branch spectra from seqID 30201034002. Note the increased strength in the iron lines and the strange feature around 3-4keV.

Initially, we believed these features may have been caused by solar activity of some sort, based on the background report for this observation from the NuSTAR website, seen in figure 11. We tried rerunning our data reduction pipeline with a stronger filter. We know our filter was applied correctly, because the data shifted around somewhat on our HID, and the exposure time was less on the filtered data set. The filter, however, had very little impact

on the shape of the spectrum 12.

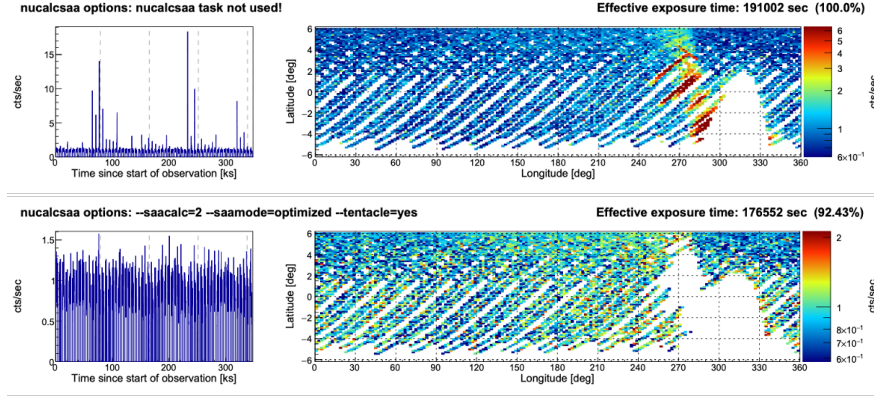


Figure 11: The unfiltered (top) and filtered (bottom) backgrounds for seqID 30201034002.

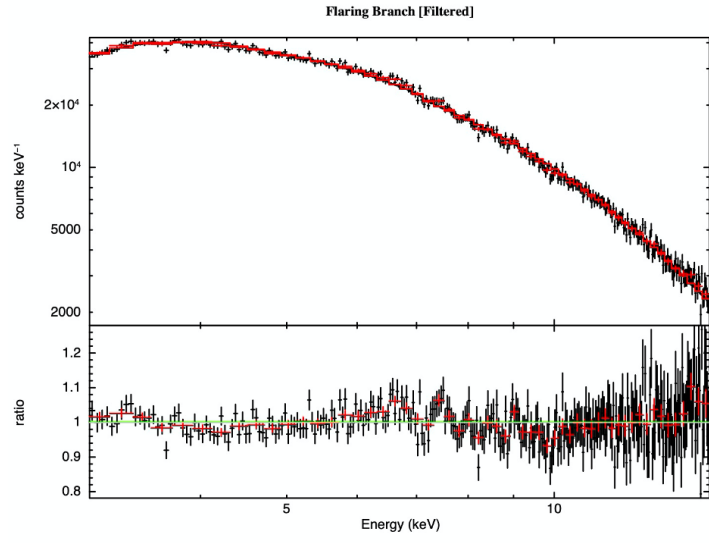


Figure 12: The flaring branch spectrum of the filtered data for seqID 30201034002. Comparing to 10, there is no discernible change in the notable features.

While the flaring branch of seqID 30201034002 does appear to have some spectral features where we would expect our iron line, it became clear that modeling these features would be particularly difficult on this data set. Due to our time constraint, we decided it would be best to continue our analysis on only the vertex sections of the two sequence IDs.

### 3.2.3 Advanced Modeling

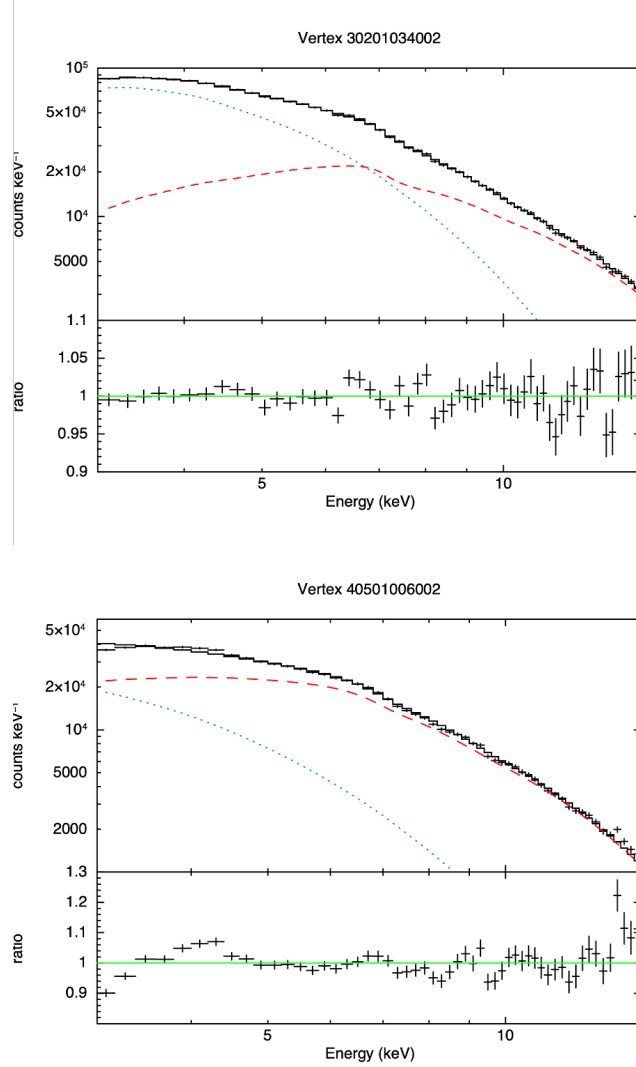


Figure 13: The final model fits and residual plots for the vertex branches of both sequence IDs. the blue (dotted) line is the disk blackbody component, and the red (dashed) line is the relxillns component. These data are optimally binned as per Kaastra and Bleeker 2016.

After creating our initial continuum models for the straylight data, we moved on to some more sophisticated modeling. We used a class of models created to model relativistic reflection in systems like this called relxill. In particular, we used the relxillns model for neutron star systems. This model is better able to fit the Fe reflection line, in order to glean some

information about the physical system based on the shape of the iron line. Along with `relxillns`, we also included a disk blackbody component in our final model, seen in fig.13.

### 3.2.4 Summary

The `relxillns` model was able to give us values for several physical parameters of the system (see tab.1). We compared these values to Ludlam et al. (2017), which looked at GX17+2 in focused observations. We found that our straylight values were in general agreement with what was in the literature, an indication of the efficacy of these straylight analyses.

Parameter	Value	Ludlam et al. (2017)
Inclination	$37.1 \pm 4.4^\circ$	$35.1(+0.2, -0.6)^\circ$
Disk Temperature	$1.5 \pm 0.2$ keV	$1.93 \pm 0.04$ keV
Inner Radius	$12.4 - 21.7$ km	$12.4 \pm 2.5$ km

Table 1: A subset of the physical parameters output by the `relxillns` model fitting

## 4 Conclusions

Between our analyses of GX5-1 and GX17+2, we have established a strong proof-of-concept for the efficacy of straylight data in the study of x-ray binary systems. For GX 5-1, we successfully recreated the analysis of Homan et al. (2018). In particular, we confirmed the conclusion that there is no apparent iron-line reflection feature to be seen from the system. For GX17+2, we successfully created physically realistic models of the emission from the vertex branch, finding parameters that are in general agreement with those in the literature. By showing that these straylight data can be used in this way, we open the door for further analysis of hundreds of serendipitous straylight observations taken over the past 8 years since NuSTAR’s launch.

## 5 Acknowledgements

This work was supported under NASA contract No. NNG08FD60C and made use of data from the NuSTAR mission, a project led by the California Institute of Technology, managed by the Jet Propulsion Laboratory, and funded by the National Aeronautics and Space Administration. We thank the NuSTAR Operations, Software, and Calibration teams for support with the execution and analysis of these observations. This research has made use of the NuSTAR Data Analysis Software (NuSTARDAS) jointly developed by the ASI Science Data Center (ASDC, Italy) and the California Institute of Technology (USA). Particular thanks to Brian Grefenstette, Renee Ludlam, and Fiona Harrison for mentoring this project.

## References

- F. Harrison, W. Craig, and F. Christensen et al. The Nuclear Spectroscopic Telescope Array (NuSTAR) High-Energy X-ray Mission. *The Astrophysical Journal*, 770:103, 2013.
- G. Hasinger and M. van der Klis. Two patterns of correlated X-ray timing and spectral behaviour in low-mass X-ray binaries. *Astronomy and Astrophysics*, 225:79–96, Nov. 1989.
- J. Homan, J. F. Steiner, D. Lin, J. K. Fridriksson, R. A. Remillard, J. M. Miller, and R. M. Ludlam. Absence of reflection features in NuSTAR Spectra of the luminous neutron star x-ray binary GX 5–1. *The Astrophysical Journal*, 853(2):157, feb 2018.
- R. M. Ludlam, J. M. Miller, M. Bachetti, D. Barret, A. C. Bostrom, E. M. Cackett, N. Degehaar, T. D. Salvo, L. Natalucci, J. A. Tomsick, F. Paerels, and M. L. Parker. A hard look at the neutron stars and accretion disks in 4u 1636-53, gx 17+2, and 4u 1705-44 with nustar. 2017.
- K. K. Madsen, F. E. Christensen, W. W. Craig, K. W. Forster, B. W. Grefenstette, F. A. Harrison, H. Miyasaka, and V. Rana. Observational Artifacts of NuSTAR: Ghost Rays and Stray Light. *arXiv e-prints*, art. arXiv:1711.02719, Nov. 2017a.

K. K. Madsen, F. E. Christensen, and W. W. Craig et al. Observational artifacts of Nuclear Spectroscopic Telescope Array: ghost rays and stray light. *Journal of Astronomical Telescopes, Instruments, and Systems*, 044003, 2017b.